Langmuir
Article
pubs.acs.org/Langmuir

Microfluidic Fabrication of Hydrogel Microparticles Containing Functionalized Viral Nanotemplates

Christina L. Lewis,[†] Yan Lin,[†] Cuixian Yang,[†] Amy K. Manocchi,[†] Kai P. Yuet,[‡] Patrick S. Doyle,[‡] and Hyunmin Yi*[,†]

[†]*Department of Chemical and Biological Engineering, Tufts University, Medford, Massachusetts 02155, and* [‡]*Department of Chemical Engineering, Massachusetts Institute of Technology, Cambridge, Massachusetts 02139*

Received June 15, 2010. Revised Manuscript Received July 7, 2010

We demonstrate rapid microfluidic fabrication of hybrid microparticles composed of functionalized viral nanotemplates directly embedded in polymeric hydrogels. Specifically, genetically modified tobacco mosaic virus (TMV) templates were covalently labeled with fluorescent markers or metalized with palladium (Pd) nanoparticles (Pd-TMV) and then suspended in a poly(ethylene glycol)-based solution. Upon formation in a flow-focusing device, droplets were photopolymerized with UV light to form microparticles. Fluorescence and confocal microscopy images of microparticles containing fluorescently labeled TMV show uniform distribution of TMV nanotemplates throughout the microparticles. Catalytic activity, via the dichromate reduction reaction, is also demonstrated with microparticles containing Pd−TMV complexes. Additionally, Janus microparticles were fabricated containing viruses embedded in one side and magnetic nanoparticles in the other, which enabled simple separation from bulk solution. These results represent a facile route to directly harness the advantages of viral nanotemplates into a readily usable and stable 3D assembled format.

Introduction

Viral assemblies have recently gained significant attention as templates for nanomaterial and device fabrication due to the highly controlled dimensions and precisely spaced functionalities conferred by chemical or biological manipulation. Examples range from spherical,[1−3] filamentous,[4−6] and rodlike[7−9] to engineered assemblies.[10,11] Particularly, tobacco mosaic virus (TMV) has been extensively studied as a nanotemplate for high capacity covalent conjugations or synthesis of metal nanoparticles[12−14] due to its well-defined and highly stable structure. Specifically, wild type TMV is a biologically occurring nanotube with 300 nm length and 18 nm diameter and consists of 2130 coat protein subunits helically wrapped around a 6.4 kb plus sense strand of genomic mRNA providing a 4 nm diameter inner channel.[15] TMV's stability spans various harsh conditions such as temperatures up to 90 °C, extreme pHs (2−10), and organic solvents (ethanol, methanol, and dimethyl sulfoxide).[8,16,17] Despite recent advances in catalytic applications[5,6,18] and 2D assembly strategies,[19−22] facile routes to assemble functionalized viral assemblies in a readily usable and stable 3D format while harnessing their unique features have not been demonstrated. This challenge arises in part from aggregation and stability issues with metal[23] and viral[24] nanoparticles. Yet, uniform distribution of functionalized viral assemblies in a stable and readily accessible 3D format providing facile handling of these hybrid nanoentities is highly desired to exploit their advantages.

Hydrogel microparticles offer highly porous 3D networks for immobilizing functionalized viral assemblies while still maintaining the function and structure of the hybrid nanostructures. Moreover, the hydrophilic nature of hydrogels should allow for a wide range of applications in aqueous environments. Additionally, microfluidics

*Corresponding author: Ph (617) 627-2195, Fax (617) 627-3991, e-mail hyunmin.yi@tufts.edu.

(1) Klem, M. T.; Young, M.; Douglas, T. *J. Mater. Chem.* **2008**, *18*(32), 3821–3823.
(2) Sapsford, K. E.; Soto, C. M.; Blum, A. S.; Chatterji, A.; Lin, T.; Johnson, J. E.; Ligler, F. S.; Ratna, B. R. *Biosens. Bioelectron.* **2006**, *21*(8), 1668–1673.
(3) Hooker, J. M.; Kovacs, E. W.; Francis, M. B. *J. Am. Chem. Soc.* **2004**, *126* (12), 3718–3719.
(4) Huang, Y.; Chiang, C.-Y.; Lee, S. K.; Gao, Y.; Hu, E. L.; Yoreo, J. D.; Belcher, A. M. *Nano Lett.* **2005**, *5*(7), 1429–1434.
(5) Nam, Y. S.; Magyar, A. P.; Lee, D.; Kim, J.-W.; Yun, D. S.; Park, H.; Pollom, T. S.; Weitz, D. A.; Belcher, A. M. *Nature Nanotechnol.* **2010**, *5*(5), 340–344.
(6) Avery, K. N.; Schaak, J. E.; Schaak, R. E. *Chem. Mater.* **2009**, *21*(11), 2176–2178.
(7) Miller, R. A.; Presley, A. D.; Francis, M. B. *J. Am. Chem. Soc.* **2007**, *129*(11), 3104–3109.
(8) Knez, M.; Sumser, M.; Bittner, A. M.; Wege, C.; Jeske, H.; Martin, T. P.; Kern, K. *Adv. Funct. Mater.* **2004**, *14*(2), 116–124.
(9) Niu, Z.; Liu, J.; Lee, L. A.; Bruckman, M. A.; Zhao, D.; Koley, G.; Wang, Q. *Nano Lett.* **2007**, *7*(12), 3729–3733.
(10) Abedin, M. J.; Liepold, L.; Suci, P.; Young, M.; Douglas, T. *J. Am. Chem. Soc.* **2009**, *131*(12), 4346–4354.
(11) Plascencia-Villa, G.; Saniger, J. M.; Ascencio, J. A.; Palomares, L. A.; Ramírez, O. T. *Biotechnol. Bioeng.* **2009**, *104*(5), 871–881.
(12) Bruckman, M. A.; Kaur, G.; Lee, L. A.; Xie, F.; Sepulveda, J.; Breitenkamp, R.; Zhang, X.; Joralemon, M.; Russell, T. P.; Emrick, T.; Wang, Q. *ChemBioChem* **2008**, *9*(4), 519–523.
(13) Lee, S.-Y.; Roysten, E.; Culver, J. N.; Harris, M. T. *Nanotechnology* **2005**, *16*(7), S435–S441.
(14) Yi, H. M.; Nisar, S.; Lee, S. Y.; Powers, M. A.; Bentley, W. E.; Payne, G. F.; Ghodssi, R.; Rubloff, G. W.; Harris, M. T.; Culver, J. N. *Nano Lett.* **2005**, *5*(10), 1931–1936.
(15) Culver, J. N. *Annu. Rev. Phytopathol.* **2002**, *40*, 287–310.
(16) Adams, M. J.; Antoniw, J. F. *Nucleic Acids Res.* **2006**, *34*(Suppl. 1), D382–385.
(17) Stubbs, G. *Semin. Virol.* **1990**, *1*, 405–412.
(18) Yang, C.; Manocchi, A. K.; Lee, B.; Yi, H. *Appl. Catal., B* **2010**, *93*(3−4), 282–291.
(19) Gerasopoulos, K.; McCarthy, M.; Banerjee, P.; Fan, X.; Culver, J. N.; Ghodssi, R. *Nanotechnology* **2010**, *21*(5), 11.
(20) Kuncicky, D. M.; Naik, R. R.; Velev, O. D. *Small* **2006**, *2*(12), 1462–1466.
(21) Lin, Y.; Balizan, E.; Lee, L. A.; Niu, Z.; Wang, Q. *Angew. Chem., Int. Ed.* **2010**, *49*(5), 868–872.
(22) Yi, H.; Rubloff, G. W.; Culver, J. N. *Langmuir* **2007**, *23*(5), 2663–2667.
(23) Campelo, J. M.; Luna, D.; Luque, R.; Marinas, J. M.; Romero, A. A. *ChemSusChem* **2009**, *2*(1), 18–45.
(24) Steinmetz, N. F.; Evans, D. J.; Lomonossoff, G. P. *ChemBioChem* **2007**, *8*(10), 1131–1136.

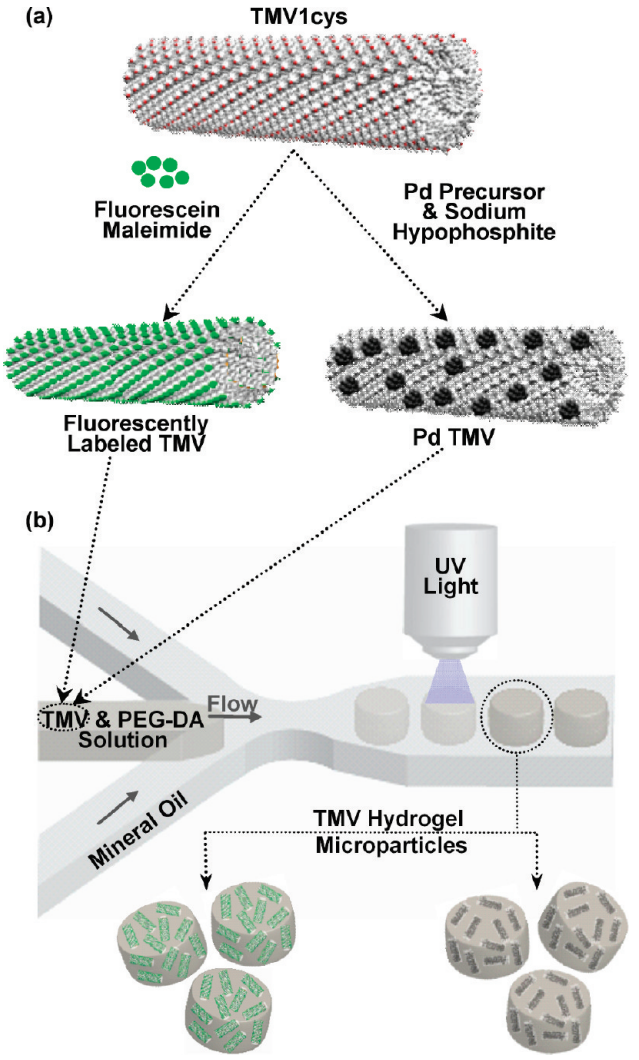

Figure 1. Fabrication procedure for microparticles containing fluorescently labeled TMV or palladium (Pd)−TMV complexes. (a) Chimera model images (Experimental Section) representing approximately one-fifth of an entire TMV1cys virion. The red dots represent cysteine residues genetically displayed on the outer surface of each coat protein (∼2130 identical proteins per virion). TMV1cys is readily labeled with fluorescein maleimide at the cysteines or metalized with Pd nanoparticles via electroless plating. (b) Schematic diagram of the microparticle fabrication procedure with a microfluidic flow-focusing device (40 × 50 μm, height × width, at the region of droplet formation). The dispersed droplet phase is a TMV−PEG solution, and the continuous phase is mineral oil. Droplets are photopolymerized with UV light providing PEG-based hydrogel microparticles (∼50 μm diameter) containing fluorescently labeled TMV or Pd−TMV complexes.

offers a rapid and efficient route to fabricate monodisperse hydrogel particles,[25] with strong potential for precise tuning of microparticle size and morphology.[26] This potential to control the structure and size of particles is important for engineering specific features, such as anisotropy, large surface areas, or light-scattering properties.[27,28] Thus, microfluidic fabrication of hydrogel microparticles provides a reproducible and consistent procedure for uniformly distributing functionalized viral assemblies in a readily usable 3D format that should address critical challenges in 3D assembly of functionalized viral hybrid nanomaterials.

In this paper, we demonstrate a microfluidic fabrication procedure to rapidly produce functionalized viral−synthetic hybrid microparticles, as shown in Figure 1. Specifically, genetically modified TMV templates (TMV1cys) are either labeled with fluorescent markers via covalent conjugation on genetically displayed cysteine groups or decorated with palladium (Pd) nanoparticles,[14,18,22,29,30] as shown in Figure 1a. Next, a microfluidic flow-focusing device is used to encapsulate functionalized TMV nanotemplates within microparticles, as shown in Figure 1b. TMV−poly(ethylene glycol) diacrylate (PEG-DA) solution is the dispersed phase in this two-phase flow process, which rapidly forms ∼500 droplets per minute within a continuous phase of mineral oil. Photopolymerization of the droplets with UV light forms PEG-based hydrogel microparticles. Fluorescently labeled TMV provides a means to evaluate the distribution of the TMV nanotemplates within the microparticles via fluorescence or confocal microscopy. Catalytic activity from the particles containing Pd−TMV complexes is demonstrated via the dichromate reduction reaction, a simple yet important model reaction for facile environmental cleanup of toxic chemicals.[18] Finally, we fabricated Janus microparticles with two sides differing in chemistry and functionality. These particles contain magnetic nanoparticles embedded in one side, which enable simple separation of the microparticles from bulk solution. Combined, these results demonstrate rapid microfluidic fabrication of functional viral−hydrogel composite microparticles enabling exploitation of nanofunctional materials, such as metal nanoparticles, in a readily deployable 3D format.

Experimental Section

TMV1cys. The creation of TMV1cys is described previously.[14] To generate concentrated TMV1cys for this work, healthy tobacco plants were infected with TMV1cys and then purified as described by Gooding et al.[31] The molecular graphic TMV base structure (PDB ID: 2tmv)[32] was obtained from the Research Collaboratory for Structural Bioinformatics Protein Data Bank (RCSB PDB, http://www.pdb.org/).[33] The TMV molecular graphic images were produced using the UCSF Chimera package from the Resource for Biocomputing, Visualization, and Informatics at the University of California, San Francisco (supported by NIH P41 RR-01081).[34−36]

TMV1cys was fluorescently labeled as described previously.[30] Briefly, purified TMV1cys was incubated at room temperature for 2 h with 10-fold molar excess of fluorescein-5-maleimide (Biotium, Hayward, CA) in 100 mM Tris buffer, pH 7.0. Sucrose gradient (pH 7.0) centrifugation, 48000*g* for 2 h, separated the fluorescein-labeled virus from unreacted fluorescein molecules. The fluorescein-labeled virus was then pelleted by centrifugation, 106000*g* for 40 min. Fluorescein-labeled and pelleted viruses were resuspended

(25) Dendukuri, D.; Doyle, P. S. *Adv. Mater.* **2009**, *21*(41), 4071–4086.
(26) Dendukuri, D.; Tsoi, K.; Hatton, T. A.; Doyle, P. S. *Langmuir* **2005**, *21*(6), 2113–2116.
(27) Hwang, D. K.; Dendukuri, D.; Doyle, P. S. *Lab Chip* **2008**, *8*(10), 1640–1647.
(28) Fujibayashi, T.; Okubo, M. *Langmuir* **2007**, *23*(15), 7958–7962.
(29) Manocchi, A. K.; Horelik, N. E.; Lee, B.; Yi, H. *Langmuir* **2010**, *26*(5), 3670–3677.
(30) Tan, W. S.; Lewis, C. L.; Horelik, N. E.; Pregibon, D. C.; Doyle, P. S.; Yi, H. *Langmuir* **2008**, *24*(21), 12483–12488.
(31) Gooding, G. V.; Hebert, T. T. *Phytopathology* **1967**, *57*(11), 1285.
(32) Namba, K.; Pattanayek, R.; Stubbs, G. *J. Mol. Biol.* **1989**, *208*(2), 307–325.
(33) Berman, H. M.; Westbrook, J.; Feng, Z.; Gilliland, G.; Bhat, T. N.; Weissig, H.; Shindyalov, I. N.; Bourne, P. E. *Nucleic Acids Res.* **2000**, *28*(1), 235–242.
(34) Couch, G. S.; Hendrix, D. K.; Ferrin, T. E. *Nucleic Acids Res.* **2006**, *34*(4), e29.
(35) Goddard, T. D.; Huang, C. C.; Ferrin, T. E. *Structure* **2005**, *13*(3), 473–482.
(36) Pettersen, E. F.; Goddard, T. D.; Huang, C. C.; Couch, G. S.; Greenblatt, D. M.; Meng, E. C.; Ferrin, T. E. *J. Comput. Chem.* **2004**, *25*, 1605–1612.

in TE buffer (10 mM Tris, pH 8.0, Sigma-Aldrich, and 1 mM EDTA, Sigma-Aldrich).

Microparticle Fabrication. Microfluidic channels were initially designed using AutoCAD 2009 (Autodesk, Inc., San Rafael, CA) and then translated into silicon master molds by the Stanford Microfluidic Foundry (http://thebigone.stanford.edu/foundry/index.html). The microchannel dimensions in the region of droplet formation was 40 × 50 μm (height × width). Poly(dimethylsiloxane) (PDMS)-based microfluidic devices were prepared by soft lithography[37] with the silicon master molds. Briefly, Sylgard 184 Silicone Elastomer by Dow Corning (Midland, MI) was poured into the silicon master mold, degassed, and cured according to the manufacturer instructions. The final thickness of the PDMS slab containing the microchannels was ~5 mm. The channels were then sealed onto PDMS-coated glass slides which were partially cured for 30 min at 65 °C and then cured for an additional 2 h at 65 °C.

The continuous phase of this two-phase microfluidic procedure was mineral oil from Sigma (St. Louis, MO) containing 3% (v/v) emulsifier, ABIL EM 90, from Evonik Industries (Parsippany, NJ). The fluorescently labeled TMV and PEG-DA solution consisted of 55% (v/v) fluorescently labeled TMV in TE buffer, 40% poly(ethylene glycol) diacrylate (PEG-DA), M_n = 700, Sigma, and 5% 2-hydroxy-2-methylpropiophenone, photoinitiator (PI), Sigma. The final concentration of fluorescently labeled TMV1cys was 0.6 mg/mL. The PEG−DA solution not containing TMV and used to form the Janus particles in Figure 3b consisted of 54% TE buffer, 39% PEG−DA, 2% blue food dye, and 5% PI. The Pd−TMV−PEG−DA solution used to form the particles shown in Figure 4c consisted of 25% PEG−DA, 15% PEG (M_w = 200), Sigma, 5% PI, and 55% Pd−TMV complex solution (3 mM sodium tetrachloropalladate(II) (Na_2PdCl_4, 99.998%, Pd precursor, Sigma), 15 mM sodium hypophosphite ($NaPH_2O_2$, precursor reducer, Sigma), and 0.3 mg/mL TMV1cys in 0.01 M phosphate buffer). The Pd−TMV−PEG−DA solution used to produce the side of the Janus particles containing Pd−TMV as shown in Figure 4f consisted of 40% PEG−DA, 5% PI, and 55% Pd−TMV complex solution as described above. The magnetic nanoparticle−PEG−DA solution used to produce the magnetic side of the Janus particles as shown in Figure 4f consisted of 40% PEG−DA, 5% PI, 25% DI water, 10% DI water containing 0.5% Tween 20, and 20% magnetic nanoparticle solution EMG-508 from Ferrotec Corp. (Bedford, NH).

The mineral oil and the preparticle solutions were separately introduced to the microchannels through 18-gauge Intramedic Luer-Stub adapters by Becton Dickinson, and Co. (Franklin Lakes, NJ) and Tygon tubing by Saint-Gobain Performance Plastics (Paris, France) connected to a common pressure source. Pressures ranging between 0 and 69 kPa were used to control the fluid flow rate through the microchannels. Type 700-BD manual pressure regulators by Control Air (Amherst, NH) and DPG1000B-30G digital pressure gauges by Omega (Stamford, CT) were used to control and monitor the pressure directed to the microchannels. The UV light source was provided by a 100 W mercury lamp and an 11000v3 UV filter set by Chroma Technology Corp. (Bellows Falls, VT). For microparticle photopolymerization within the PDMS microchannels, UV light was focused onto a specific location within the channel through an Olympus (Center Valley, PA) long working distance 20× objective with a NA of 0.4 on an Olympus BX51 upright microscope.

Following photopolymerization, the microparticles are collected in reservoirs located at the end of the microchannels. The particles were transferred from this reservoir into an Eppendorf tube with a pipet. The particles were briefly centrifuged to separate them from the mineral oil and remaining PEG monomer solution. The particles were then removed from the bottom of the Eppendorf tube with a pipet, transferred to a new tube, and

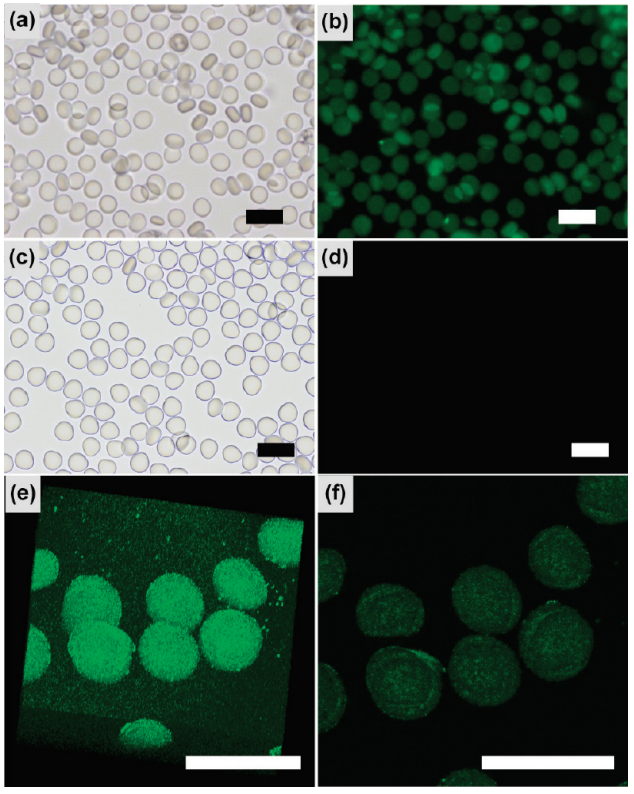

Figure 2. Microparticles containing fluorescently labeled TMV nanotemplates. (a, c) Bright-field and (b, d) fluorescence micrographs of microparticles with and without fluorescently labeled TMV, respectively. (e) Reconstituted 3-D and (f) center *z*-scan confocal images of microparticles containing fluorescently labeled TMV. The scale bars represent 100 μm.

washed several times with DI water containing 0.5% (v/v) Tween 20 (Sigma, St. Louis, MO). The washing procedure consisted of pipetting the DI water solution into the tube containing the particles, vortexing, and centrifugation before removing the DI water supernatant.

Imaging. Bright-field and fluorescence micrographs were captured with an Olympus (Center Valley, PA) BX51 upright microscope equipped with an Olympus DP70 microscope digital camera and a standard green filter set, 31001 from Chroma Technology Corp. (Bellows Falls, VT). Confocal images were acquired on a Leica DMIRE2 microscope with a TCS SP2 scanner (Wetzlar, Germany) equipped with a 63× (NA 1.2) water immersion objective and analyzed at 488 nm excitation and 500−530 nm emission. Confocal image analysis was performed with the Leica Confocal software (Wetzlar, Germany). A series of *z*-scan images with a depth scan increment of 3 μm were collected from the ~40 μm thick cross section of the disk-shaped microparticles containing fluorescently labeled TMV. Compilation of this image series provided a reconsitutued 3-D image, as shown in Figure 2e. The *z*-scan image captured at the particle center is shown in Figure 2f. Transmission electron microscope (TEM) images were collected using a JEOL 2100 TEM operated at 200 kV. TEM samples were prepared by placing the Pd−TMV complex solution on a TEM grid and allowing the solution to settle for 2 min. The grid was then placed on filter paper to wick away the liquid.

Catalytic Activity for Dichromate Reduction. The reaction conditions and the procedure for determining the conversion and apparent first-order rate constant for dichromate reduction were followed as described previously.[18] Briefly, the 0.3 mL reaction solutions consisted of 0.1 mM potassium dichromate ($K_2Cr_2O_7$, 99.5%, Sigma, St. Louis, MO), which was the source of Cr(VI), and 100 mM sodium formate (HCOONa, 99%, Fisher), which

(37) McDonald, J. C.; Duffy, D. C.; Anderson, J. R.; Chiu, D. T.; Wu, H.; Schueller, O. J. A.; Whitesides, G. M. *Electrophoresis* **2000**, *21*(1), 27–40.

was the electron donor for the dichromate reduction. The ionic equations for the redox reaction are shown in eqs 1 and 2.[38]

$$Cr_2O_7^{2-} + 14H_3O^+ + 6e^- \leftrightarrow 2Cr^{3+} + 21H_2O \quad (1)$$

$$HCOO^- + H_2O \leftrightarrow CO_2 + H_3O^+ + 2e^- \quad (2)$$

The dichromate reduction reactions were carried out in Eppendorf tubes with continuous stirring. At specific time points, samples of the reaction supernatant were evaluated at 350 nm, characteristic of the adsorption of Cr(VI) ions, with an Evolution 300 UV−vis spectrophotometer (Thermo Scientific, Waltham, MA) to determine the concentrations of Cr(VI). The extent of the catalytic reduction, expressed as percent conversion, was determined with eq 3, where $[Cr(VI)]_0$ represents the initial concentration and [Cr(VI)] represents the concentration at a specific time point.

$$\text{conversion } (\%) = \frac{[Cr(VI)]_0 - [Cr(VI)]}{[Cr(VI)]_0} \times 100 \quad (3)$$

On the basis of the large concentration difference between sodium formate and potassium dichromate, the sodium formate concentration was assumed constant throughout the reaction period. Thus, the reaction of eqs 1 and 2 followed pseudo-first-order kinetics. A first-order rate constant, as shown in eq 4, was estimated via the linear regression of $\ln([Cr(VI)]/[Cr(VI)]_0)$ vs reaction time, as shown in eq 5.

$$r = -\frac{d[Cr(VI)]}{dt} = k_1[Cr(VI)] \quad (4)$$

$$\ln \frac{[Cr(VI)]}{[Cr(VI)]_0} = -k_1 t \quad (5)$$

Results and Discussion

Microfluidic Fabrication of Fluorescently Labeled TMV−PEG Microparticles. We first demonstrate rapid microfluidic fabrication of viral−synthetic hybrid microparticles as shown in Figure 2. For this, TMV1cys was fluorescently labeled at the genetically displayed cysteine residues via covalent conjugation with thiol−reactive fluorescein maleimide (Figure 1a). The labeled TMVs were then purified using sucrose gradient centrifugation[30] and mixed with PEG−DA solution. TMV−PEG particles were formed by a continuous microfluidic procedure with a poly(dimethylsiloxane) (PDMS)-based flow-focusing device (FFD) and UV photopolymerization, as shown in Figure 1b. The bright-field and fluorescence micrographs of Figure 2a,b show the formation of highly uniform microparticles as well as uniform distribution of TMV within the particles (~50 pg of TMV per particle). Importantly, the images of particles without fluorescently labeled TMV in Figure 2c,d do not show fluorescence, confirming that the fluorescence in Figure 2b is from fluorescently labeled TMV. While the conditions employed in this study consistently produced ~50 μm diameter particles, there are various means to control droplet sizes in FFDs (see ref 39 for a thorough review on this subject). Briefly, the droplet size is largely dictated by dimension of the channel supplying the monomer stream, and larger flow rates in the focusing mineral oil will lead to smaller droplets. Confocal microscopy was next employed to evaluate the dispersion of TMV throughout the particles. Both the reconstituted 3-D and *z*-scan

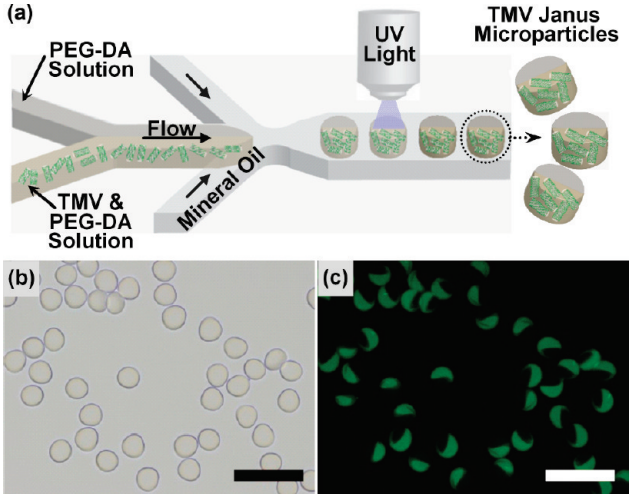

Figure 3. Microfluidic fabrication of Janus microparticles containing fluorescently labeled TMV nanotemplates. (a) Schematic diagram of Janus particle synthesis in a microfluidic flow-focusing device. (b) Bright-field and (c) fluorescence micrographs of Janus microparticles with one side of the particles containing fluorescently labeled TMV.

(captured at the particle center) images of the TMV-encapsulated microparticles in Figure 2e,f confirm uniform distribution of TMVs throughout the microparticles. Combined, these results illustrate rapid microfluidic fabrication of hybrid microparticles containing fluorescently labeled TMV nanotemplates that are uniformly distributed throughout PEG matrices via FFD droplet-based particle formation.

Fabrication of Janus Microparticles with Fluorescently Labeled TMV. Next, we demonstrate fabrication of Janus microparticles containing fluorescently labeled TMV nanotemplates, as shown in Figure 3. A microfluidic FFD specific for the fabrication of Janus microparticles contains two separate polymer streams that form each side of the Janus particles, as illustrated in the schematic diagram of Figure 3a. For this study, one stream contained PEG−DA solution while the other contained fluorescently labeled TMV within PEG−DA solution. The Janus particle fabrication procedure takes advantage of laminar flow by photopolymerizing the Janus droplets before significant mixing occurs within the droplets. The bright-field micrograph of Figure 3b shows Janus particles with equally consistent particle fabrication similar to that for the non-Janus particles shown in Figure 2a,c. The fluorescence micrograph of Figure 3c clearly shows that only one side of the Janus particles contains uniform fluorescence. This result confirms both spatial confinement and uniform distribution of the encapsulated TMV afforded by the laminar nature of the microfluidic flow. Combined with the generality of this covalent conjugation scheme of the fluorescent marker molecules (e.g., rhodamine,[14] Cy3 and Cy5,[22] and fluorescein[30]) to the cysteines, the result shown here suggests a simple means to fabricate hybrid particles with multiple small molecule components in spatially discrete regions within a single entity. Overall, this result demonstrates rapid and consistent fabrication of Janus particles as well as the ability to form multifunctional particles with discrete regions of encapsulated TMV nanotemplates.

Fabrication of Microparticles with Pd−TMV Complexes. As shown in Figure 4, we next demonstrate rapid microfluidic fabrication of hybrid microparticles with TMV-templated palladium (Pd) nanoparticles directly embedded in the PEG-based polymer matrix. Parts a and b of Figure 4 show TEM images of Pd nanoparticles formed with and without TMV1cys nanotemplates,

(38) Vincent, T.; Guibal, E. *Ind. Eng. Chem. Res.* **2002**, *41*(21), 5158–5164.
(39) Christopher, G. F.; Anna, S. L. *J. Phys. D: Appl. Phys.* **2007**, *40*(19), R319–R336.

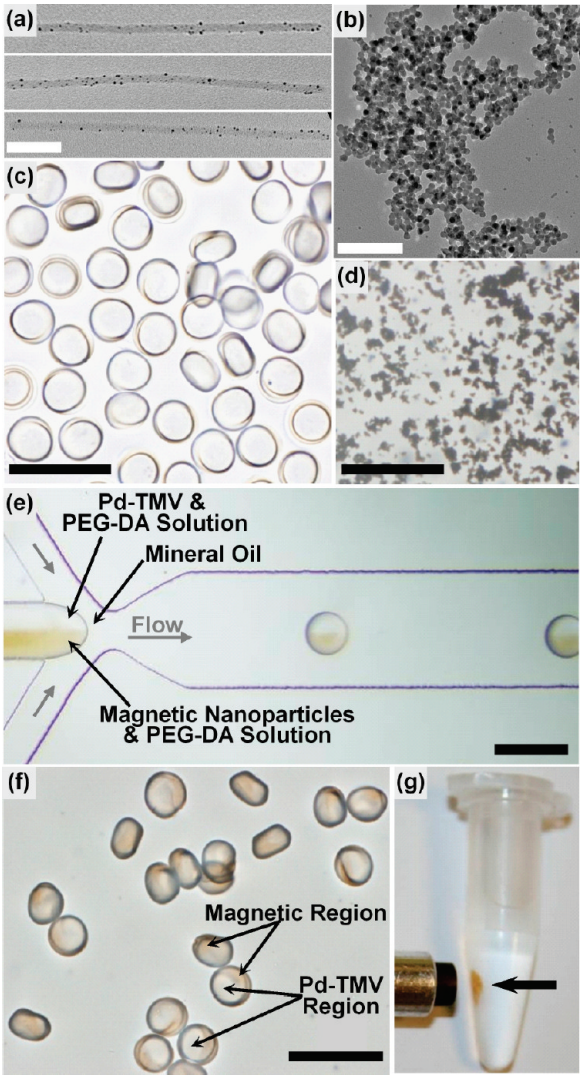

Figure 4. Microfluidic fabrication of palladium (Pd)−TMV−PEG−hybrid microparticles. TEM images of Pd nanoparticles formed (a) on TMV1cys nanotemplates and (b) in bulk solution without TMV. Bright-field micrographs of (c) microparticles containing Pd−TMV complexes, (d) Pd nanoparticle aggregates in a microfluidic device, (e) microfluidic flow-focusing device (FFD) specific for fabrication of Janus microparticles, and (f) Janus microparticles containing Pd−TMV and magnetic nanoparticles. (g) Photograph of Janus particles attracted to a small magnet. The white scale bars in (a) and (b) represent 100 nm, and the black scale bars in (c) to (g) represent 100 μm.

respectively, under identical conditions of 3 mM Pd precursor and 15 mM hypophosphite reducer. Average particle sizes are drastically different in these two cases (5 nm versus 10 nm), clearly demonstrating the utility of TMV templates, which provide ample adsorption sites for particle nucleation leading to substantially smaller particles.[13] Furthermore, the Pd nanoparticles spontaneously aggregated (Figure 4b) in the absence of TMV1cys nanotemplates or surfactants under the synthesis conditions employed. Meanwhile, Pd−TMV complexes remained well-dispersed, and the TMV1cys nanotemplates maintained their overall tubular structure. In addition, the Pd−TMV complex has shown to be highly stable through extensive rinsing, drying, and prolonged storage under ambient conditions.[29]

The bright-field micrograph of Figure 4c shows PEG hydrogel microparticles containing Pd−TMV complexes (~25 pg TMV per particle) with high consistency and uniformity similar to fluorescein-conjugated TMV−PEG particles (Figures 2a and 3b). Meanwhile, Figure 4d shows that Pd−PEG mixtures without TMV templates quickly precipitated and clogged the microfluidic device before photopolymerization. This observation further confirms the advantage of TMV as a nanotemplate, which enables uniform distribution of the Pd nanoparticles within the microparticles without any visible phase segregation.

In Figure 4e−g, we demonstrate multifunctional capability of Janus microparticles containing Pd−TMV and magnetic nanoparticles in two distinct phases. A microfluidic FFD containing two separate streams of different polymer solutions for fabrication of Janus particles (Figure 3a) was employed to coflow Pd−TMV−PEG−DA solution and a magnetic nanoparticle−PEG−DA solution to form droplets. As shown in Figure 4e, the laminar nature of the microfluidic flow enables the Pd−TMV−PEG−DA stream (clear) and magnetic−PEG−DA stream (brown) to remain separated. These droplets were photopolymerized with UV light to form multifunctional Janus microparticles as shown Figure 4f.

While the Janus particle symmetry does not remain consistent throughout polymerization, each polymer phase containing Pd−TMV or magnetic nanoparticles remains as discrete regions within the particles, as indicated by the arrows in Figure 4f. We believe this subtle flaw rises from a difference in the rate of polymerization between the two streams. Importantly, these Janus microparticles can provide a multifunctional capability that combines the potential applications of Pd−TMV and magnetic nanoparticles in one entity. For example, Figure 4g shows simple magnetic separation of these particles via the magnetic nanoparticles within the hydrogel matrix on one side of the particles. Overall, these results demonstrate rapid fabrication of uniform PEG microparticles containing Pd−TMV as well as magnetic nanoparticles via direct embedding with a microfluidic FFD.

Catalytic Activity of Pd−TMV−PEG Hybrid Microparticles. Finally, we examine the catalytic activity of Pd−TMV complexes encapsulated in PEG microparticles for the dichromate reduction reaction as shown in Figure 5. Different quantities of microparticles containing Pd−TMV complexes were resuspended into 0.3 mL reaction mixtures of 0.1 mM dichromate, the source of Cr(VI), and 100 mM sodium formate, the electron donor for dichromate reduction, to carry out the reaction. A UV−vis spectrophotometer was employed to monitor the reaction at 350 nm, the absorption maximum of dichromate ion as previously reported.[18] The conversion of dichromate catalyzed by microparticles with a range of Pd loading (1−3 μg) was determined over a 1 h time period, as shown in Figure 5a. Microparticles with the largest quantity of Pd (3.1 μg) yielded 92% conversion within 30 min and reached near-complete conversion within 1 h. Meanwhile, lower Pd loading yielded slower conversion as expected. Furthermore, Pd−TMV microparticles containing 2 μg of Pd and aged for 1 week in ambient conditions exhibited comparable conversion to freshly prepared particles, strongly indicating the stability of the microparticles. The bottom two curves in Figure 5a show that both negative control samples (TMV−PEG and PEG microparticles) yielded no catalytic activity under the conditions examined. This clear difference in the conversion rate demonstrates the catalytic activity of the microparticles containing Pd−TMV.

To further quantify the catalytic activity versus Pd amount, a first-order kinetics analysis was conducted to determine the reaction rate constants, k (min^{-1}), as previously reported.[18] As shown in Figure 5b, the reaction rate constants exhibited a linear relationship to the Pd loading amount. In addition, all of the conditions examined strictly followed simple first-order batch

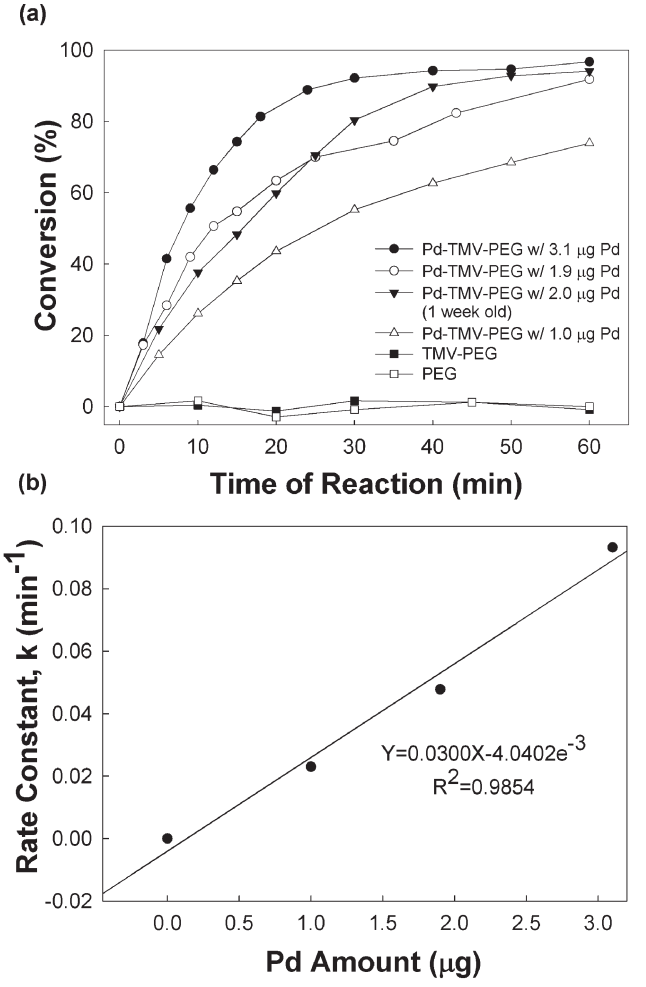

Figure 5. Catalytic activity of PEG microparticles containing Pd−TMV complexes for dichromate reduction. (a) Conversion of dichromate catalyzed by microparticles containing 1−3 μg of Pd from the Pd−TMV complexes. (b) Plot of first-order reaction rate constants, k (min^{-1}), versus the total quantity of Pd within the microparticles from the Pd−TMV complexes. Straight line represents data fitting result from the linear regression.

reaction kinetics (data not shown), suggesting the utility of microparticle carriers for controlled catalyst loading. Furthermore, the rate constants shown in Figure 5b exhibit comparable or higher values than surface-displayed Pd particles reported in our previous study,[18] suggesting uniform distribution of Pd−TMV complexes that appeared to be readily accessible to the reactants. In summary, the dichromate reduction reaction study demonstrates the catalytic activity and stability of microparticles containing Pd−TMV complexes. These results indicate that the microparticles provide a stable and simple-to-handle carrier for Pd−TMV complexes while the TMV nanotemplates provide a platform for facile synthesis and dispersion of small and catalytically active Pd nanoparticles.

Conclusions

Viruses have been increasingly recognized as useful and robust templates for nanomaterial fabrication. Functionalized viral assemblies may include a variety of covalent conjugations or metal nanoparticles. A current challenge is to distribute functionalized viral assemblies in a readily usable 3D format while minimizing aggregation and stability issues commonly confronted with metal and viral nanoparticles. For this study, we presented a procedure for addressing this challenge by encapsulating functionalized TMV nanotemplates in hydrogel microparticles. These particles offer highly porous 3D networks for immobilizing functionalized viral assemblies while still maintaining the function and structure of the hybrid nanostructures. Additionally, microfluidics offers an efficient route to rapidly fabricate monodisperse hydrogel particles along with the ability to precisely tune microparticle size and morphology.

To generate the viral−synthetic hybrid microstructures, droplets of functionalized TMV nanotemplates suspended in a PEG−DA solution were first formed with a microfluidic flow-focusing device and then photopolymerized with UV light to form microparticles. Uniform distribution of TMV nanotemplates throughout the microparticles was confirmed with fluorescence and confocal microscopy images of microparticles containing fluorescently labeled TMV. The functionality of TMV nanotemplates following encapsulation within microparticles was also confirmed through the dichromate reduction reaction, where microparticles containing Pd−TMV complexes provided catalytic activity. Finally, the potential fabrication of multifunctional microparticles was illustrated through Janus microparticle formation, which contained magnetic nanoparticles embedded in one side. It was shown that these Janus particles could be easily separated from bulk solution with a magnet. Overall, these results demonstrate a method for immobilizing functional viral assemblies in a readily usable and stable 3D format. Combined with enhanced thermostability of Pd−TMV complexes,[40] this fabrication method presents robust and stable viral−synthetic hybrid entities offering unique advantages in applications such as catalysis or biosensing where well-dispersed and readily accessible functionalities from nanomaterials are highly desired.

Acknowledgment. We gratefully acknowledge financial support by the Stanley Charm Fellowship (C.Y.). Partial funding for this work was also provided by the National Science Foundation under Grants CBET-0941538, DMR-1006613, and DMR-1006147 as well as Award K12GM074869 (TEACRS) from the National Institute of General Medical Sciences (Y.L). The content is solely the responsibility of the authors and does not necessarily represent the official views of the National Institute of General Medical Sciences or the National Institutes of Health. This work was also performed in part at the Center for Nanoscale Systems (CNS) at Harvard University, a member of the National Nanotechnology Infrastructure Network (NNIN) supported by the National Science Foundation (Award ECS-0335765).

(40) Manocchi, A. K.; Seifert, S.; Lee, B.; Yi, H. *Langmuir* **2010**, *26*(10), 7516–7522.